

# Photon-assisted Landau-Zener transition: Role of coherent superposition states

Zhe Sun,<sup>1,2,\*</sup> Jian Ma,<sup>1,3</sup> Xiaoguang Wang,<sup>1,3</sup> and Franco Nori<sup>1,4</sup>

<sup>1</sup>*Advanced Science Institute, RIKEN, Wako-shi, Saitama 351-0198, Japan*

<sup>2</sup>*Department of Physics, Hangzhou Normal University, Hangzhou 310036, China*

<sup>3</sup>*Zhejiang Institute of Modern Physics, Department of Physics, Zhejiang University, Hangzhou 310027, China*

<sup>4</sup>*Physics Department, The University of Michigan, Ann Arbor, Michigan 48109-1040, USA*

We investigate a Landau-Zener (LZ) transition process modeled by a quantum two-level system (TLS) coupled to a photon mode when the bias energy is varied linearly in time. The initial state of the photon field is assumed to be a superposition of coherent states, leading to a more intricate LZ transition. Applying the rotating-wave approximation (RWA), analytical results are obtained revealing the enhancement of the LZ probability by increasing the average photon number. We also consider the creation of entanglement and the change of photon statistics during the LZ process. Without the RWA, we find some qualitative differences of the LZ dynamics from the RWA results, e.g., the average photon number no longer monotonically enhances the LZ probability. The ramifications and implications of these results are explored.

PACS numbers: 03.65.Ud, 03.65.Yz

## I. INTRODUCTION

Landau-Zener (LZ) transitions involve a quantum two-level system (TLS) with a constant coupling strength  $\Delta$  between two adiabatic energy levels. A control parameter is swept at a constant velocity  $v$ , so that an avoided crossing of energy levels occurs, and provides the probability that the system will stay in an adiabatic state. LZ transitions have attracted considerable attention theoretically (see, e.g., Refs. [1–6]) and experimentally (see, e.g., Refs. [7–9]).

In a variety of physical areas, LZ processes play an important role, e.g., in artificial atoms [10] and Bose-Einstein condensates in optical lattices [11]. Especially in superconducting circuits which can behave like controllable quantum TLSs [12–15], LZ and Landau-Zener-Stückelberg (LZS) problems have been studied by several groups [1, 16–21]. The standard LZ problem for an isolated TLS can be solved exactly. For some many-level systems, the LZ transition probability can also be calculated exactly for some initial states [22–24]. LZ transitions controlled by classical fields are considered in Ref. [25], and in a quantum photon field the authors of Ref. [26] found that varying the LZ sweep rate produces collapses and revivals of the coherent field amplitude.

Naturally, a quantum TLS is influenced by its environment, and therefore there have been many studies about the dissipative LZ problem. Exact results are available at zero temperature [27, 28], and various numerical methods have been employed to study the cases at finite temperatures [29–31]. The nonmonotonic dependence of the LZ probability on the sweep velocity was studied in Ref. [29] using numerical methods. Environment parameters, such as temperature, can exponentially enhance the coherent oscillations generated at a LZ transition [31].

It is interesting to replace the classical coupling  $\Delta$  by a fully quantum-field coupling; then the TLS and the field form a whole composite quantum system. In this paper we consider a quantum TLS coupled to a photon mode when the bias energy is varied linearly in time.

Coherent superpositions of coherent states, like  $|\psi(0)\rangle_{\text{ph}} = (|\alpha\rangle + e^{i\theta} |-\alpha\rangle) / N_\theta$ , with the normalization constant  $N_\theta^2 = 2(1 + \cos\theta e^{-2|\alpha|^2})$ , have attracted extensive interest as a distinct class of nonclassical states with interesting properties. For a large amplitude  $\alpha$ , these can be interpreted as quantum superpositions of two macroscopically-distinguishable states, the so-called Schrödinger cat states. Such states can be prepared in various systems and play an important role in fundamental tests of quantum theory and in many quantum-information-processing tasks [32–34], including quantum computation [35], quantum teleportation [36], and precision measurements [37, 38].

We aim to discover the effect of the initial superposition of coherent states on the LZ transition. The increasing average photon number may enhance the LZ probability. We also focus on the effect of the LZ process on the quantum properties of the whole system, including entanglement creation and changing the photon distribution.

By applying a rotating-wave approximation (RWA), we obtain analytical results which reveal the enhancement of the LZ probability when increasing the average photon number. Whereas, without the RWA we find some qualitative differences of the LZ dynamics from the RWA results; e.g., there are two stages of the LZ transition and the final LZ probability no longer monotonically depends on the average photon number.

This paper is organized as follows. In Sec. II, we introduce the standard LZ model and the quantized LZ model considered in this paper. In Sec. III, by employing the RWA, we analytically calculate the LZ probability, the entanglement between the TLS and the field, and the photon statistics characterized by the Mandel parameter

---

\*Electronic address: [sunzhe@hznu.edu.cn](mailto:sunzhe@hznu.edu.cn)

*Q.* Numerical results are shown in this section to confirm the analytical results. In Sec. IV, *without* the RWA, numerical and analytical results are given to compare with the RWA results. The thermal state of the photon field is also considered, in order to compare with the case of a superposition of coherent states in which the photon distribution is Poissonian. Finally, we present the conclusions.

## II. HAMILTONIAN OF THE LANDAU-ZENER TRANSITION

Let us first briefly gather together several results that will be used in this work. The standard LZ problem, for an isolated quantum TLS driven by a *classical* field, is described by the Hamiltonian

$$H = -\frac{vt}{2}\sigma_z - \frac{\Delta}{2}\sigma_x, \quad (1)$$

in terms of the Pauli matrices  $\sigma_{x,z}$ , and  $\sigma_x = \sigma_+ + \sigma_-$  ( $\hbar = 1$  is assumed throughout). Let the states  $|\uparrow\rangle$  and  $|\downarrow\rangle$  denote the eigenstates of  $\sigma_z$ , i.e., the so-called diabatic states with energies  $\pm vt/2$  which cross at  $t = 0$ . The constant  $v$  is the sweep velocity, by which the energies of the diabatic states cross. The coupling  $\Delta$  denotes the interaction between the two diabatic states, which are chosen to be positive and time independent. For  $\Delta \neq 0$ , the diabatic states are not eigenstates of the Hamiltonian in Eq. (1), and the avoided-level crossing appears between the adiabatic energies  $E_{\pm}(t) = \pm \left[ (vt)^2 + \Delta^2 \right]^{1/2} / 2$  at  $t = 0$ . Thus, generally, a population transfer is induced. Asymptotically, for times  $|t| \gg \Delta/v$ , the diabatic states coincide with the adiabatic states. The LZ problem asks for the probability of the TLS ending up in the initially unoccupied level, and is given by  $P_{0,LZ} = 1 - \exp(-\pi\Delta^2/2v)$ , which is an exact result for all  $\Delta$  and  $v$ . In the adiabatic limit  $\Delta^2/v \gg 1$ , i.e., when the sweep occurs slowly enough,  $P_{0,LZ}$  will saturate at 1, which implies that the transfer of population between the adiabatic eigenstates is prevented by the splitting  $\Delta$ .

In this work we consider a *quantized* LZ Hamiltonian describing the coupling of a quantum TLS to a single-photon-field mode. The Hamiltonian reads

$$H = \frac{\omega_0}{2}\sigma_z + \omega a^\dagger a - \frac{vt}{2}\sigma_z - \frac{\Delta}{2}\sigma_x (a + a^\dagger), \quad (2)$$

where the operator  $a$  ( $a^\dagger$ ) annihilates (creates) a photon in the field mode with frequency  $\omega$ , and the energy bias of the TLS is denoted by  $\omega_0$ . In this paper, the resonance case  $\omega_0 = \omega$  is considered. Hence we rewrite the total Hamiltonian in a rotating frame defined by the operator  $\hat{N} = a^\dagger a + \sigma_z/2$ , at the frequency  $\omega$ .

In the weak-coupling regime, where the coupling is at least an order of magnitude less than the energy frequency, i.e.,  $\Delta < 0.1\omega$ , one can employ a RWA, and the

Hamiltonian becomes

$$H = -\frac{vt}{2}\sigma_z - \frac{\Delta}{2}(a\sigma_+ + a^\dagger\sigma_-). \quad (3)$$

Now the system is modeled in terms of a time-dependent Jaynes-Cummings Hamiltonian [26, 39, 40], which can also be called the Landau-Zener-Jaynes-Cummings (LZ-JC) model. Note that the operator  $\hat{N} = a^\dagger a + \sigma_z/2$  is conserved by this Hamiltonian.

When considering a finite detuning  $\delta\omega = \omega_0 - \omega$ , the RWA is usually justified in the condition that  $|\delta\omega| \ll \omega_0 + \omega$ . Then a constant energy bias  $\delta\omega$  is added to the adiabatic states, and the LZ-JC Hamiltonian becomes  $H = -\frac{vt-\delta\omega}{2}\sigma_z - \frac{\Delta}{2}(a\sigma_+ + a^\dagger\sigma_-)$ . The finite detuning  $\delta\omega$  gives no change to the LZ process except translating the time when the LZ transition occurs, from  $t = 0$  to  $t = \delta\omega/v$ .

This kind of model was considered in Ref. [39], where highly nonclassical sub-Poissonian states were found. Some later work [23, 40] mentioned the LZ problem in the JC and Rabi models. A superconducting qubit coupled to a transmission-line resonator [41] can be described by the quantized LZ Hamiltonian in Eqs. (2) and (3) when the transition frequency of the charge (flux) qubit is varied linearly in time by a driving charge (magnetic flux). Furthermore, in this kind of circuit quantum electrodynamics, the strong coupling can be obtained, which allows the cases beyond the RWA [42].

## III. LANDAU-ZENER TRANSITION PROCESSES, ENTANGLEMENT CREATION AND PHOTON DISTRIBUTION WITH THE RWA

Let us assume that the initial state of the total system is in a direct product form, and the TLS initially starts from  $|\uparrow\rangle$  and that the photon field starts from a Fock state, then the initial state of the whole system  $|\psi(0)\rangle_{\text{tot}} = |\uparrow\rangle \otimes |n\rangle$ . Under the LZ-JC Hamiltonian in Eq. (3), the state at time  $t$  becomes

$$|\psi(t)\rangle_{\text{tot}} = A_n(t)|\uparrow n\rangle + B_n(t)|\downarrow n+1\rangle, \quad (4)$$

where, the time-dependent coefficients  $A_n(t)$  and  $B_n(t)$  are the solutions of a second-order Weber equation and in the form of combinations of parabolic cylinder functions [1]. Explicitly, the coefficients

$$\begin{aligned} A_n(t) &= \sum_{\pm} \mu_{n,\pm} D_{-1-i\delta_n}(\pm Z_t), \\ B_n(t) &= \sum_{\pm} \nu_{n,\pm} D_{-i\delta_n}(\pm Z_t), \end{aligned} \quad (5)$$

where  $D_{-1-i\delta_n}(\pm Z_t)$  [ $D_{-i\delta_n}(\pm Z_t)$ ] are the parabolic cylinder functions and the parameters  $Z_t = -\sqrt{2}e^{i\pi/4}\sqrt{v/2t}$  and  $\delta_n = \Delta^2(n+1)/(4v)$ , because when the field mode is occupied by  $n$  photons,

the splitting  $\Delta$  is enhanced by a factor  $\sqrt{n+1}$ , as compared with the standard LZ model. The parameters  $\nu_{n,\pm}$  and  $\mu_{n,\pm}$  satisfy  $\nu_{n,\pm} = \mp\mu_{n,\pm}e^{-i\pi/4}/\sqrt{\delta_n}$ . Moreover, if the bias energy  $vt_0$  is finite, then we have  $\mu_{n,+} = D_{-i\delta_n}(-Z_{t_0})/[D_{-i\delta_n}(-Z_{t_0})D_{-1-i\delta_n}(Z_{t_0}) + D_{-i\delta_n}(Z_{t_0})D_{-1-i\delta_n}(-Z_{t_0})]$  and  $\mu_{n,-} = \mu_{n,+}D_{-i\delta_n}(Z_{t_0})/D_{-i\delta_n}(-Z_{t_0})$ . Usually, one considers the limit cases when the bias energy  $vt$  is switched from a large negative value to a large positive value; then with the asymptotes of the parabolic cylinder functions, we find  $A_n(t) \approx \exp(-\pi\delta_n)$ , which implies that for an initial state  $|\uparrow n\rangle$ , the final probability of the TLS staying in  $|\uparrow\rangle$  is  $P_{\uparrow,n} = P_{\uparrow,0} \exp(-\pi\Delta^2 n/2v)$ , with  $P_{\uparrow,0} = \exp(-\pi\Delta^2/2v)$  denoting the vacuum case.

When the initial state of the field is a superposition of Fock states, the initial state of the whole system reads

$$|\psi(0)\rangle_{\text{tot}} = |\uparrow\rangle \otimes \sum_{n=0}^{\infty} C_n |n\rangle, \quad (6)$$

where the superposition parameter  $C_n$  satisfies  $\sum_{n=0}^{\infty} |C_n|^2 = 1$ . Then, multi level LZ transitions are expected at the avoided-level crossings of the diabatic energy levels, and we sketch the energy-level diagram in Fig. 1 (a). The final probability of the TLS staying in  $|\uparrow\rangle$  becomes an average of  $P_{\uparrow,n}$ , and then the final LZ transition probability at  $t = \infty$  reads

$$P_{\text{LZ}}(\infty) = 1 - P_{\uparrow,0} \sum_{n=0}^{\infty} |C_n|^2 \exp\left(-\frac{\pi\Delta^2 n}{2v}\right). \quad (7)$$

### A. LZ processes for coherent superposition states

Hereafter we focus on the nonclassical properties associated with the following superposition of coherent states:

$$|\psi(0)\rangle_{\text{ph}} = \frac{1}{N_{\theta}} (|\alpha\rangle + e^{i\theta} |-\alpha\rangle), \quad (8)$$

where  $N_{\theta}^2 = 2(1 + \cos\theta e^{-2|\alpha|^2})$  is a normalization constant and, for simplicity, we assume  $\alpha$  to be real. Such states are superpositions of classically distinguishable states and involve fundamentally nonclassical properties. Therefore, they are important for investigating fundamental tests of quantum theory and in many quantum information processing tasks [32–34].

As shown in Refs. [43, 44], for an anharmonic oscillator with the Hamiltonian  $H = v(a^\dagger a + \frac{1}{2}) + \chi(a^\dagger a)^2$ , an initial coherent state  $|\alpha\rangle$  will evolve into the coherent superposition states in Eq. (8) with a superposition phase  $\theta$  corresponding to different evolution times. And at some special time such as  $t = \pi/(2\chi)$ , the so-called ‘‘Yurke-Stoler’’ coherent state with  $\theta = \pi/2$  can be achieved. In an optical system, the coherent superposition states with large amplitude can be generated by using homodyne detection and photon number states as resources [34], and the superposition phase  $\theta$  is related to the photon numbers.

Recalling the initial state in Eq. (6), the superposition coefficient becomes

$$C_n = \frac{1}{N_{\theta}} \exp\left(-\frac{|\alpha|^2}{2}\right) \frac{\alpha^n [1 + (-1)^n]}{\sqrt{n!}}. \quad (9)$$

It follows that we can calculate the final LZ transition probability exactly

$$P_{\text{LZ}}(\infty) = 1 - \frac{2P_{\uparrow,0}}{N_{\theta}^2 e^{|\alpha|^2}} \left( e^{|\alpha|^2 P_{\uparrow,0}} + \cos\theta e^{-|\alpha|^2 P_{\uparrow,0}} \right). \quad (10)$$

It turns out that  $P_{\text{LZ}}(\infty)$  now depends on the initial conditions  $|\alpha|^2$  and  $\theta$ ; the former is associated with the average photon of field and the latter determines the types of superpositions. Obviously, for  $|\alpha|^2 = 0$  and  $\cos\theta \neq -1$ , then  $P_{\text{LZ}}(\infty) = 1 - P_{\uparrow,0}$ , corresponding to the standard LZ probability. Whereas in the limit  $|\alpha|^2 \rightarrow \infty$ , with finite ratio  $\Delta^2/v \neq 0$ ,  $P_{\text{LZ}}(\infty)$  will tend to unity monotonically.

#### 1. Yurke-Stoler state

When  $\theta = \pi/2$ , the superposition state is the so-called Yurke-Stoler (YS) coherent state [43]:  $|\alpha\rangle_{\text{YS}} = (|\alpha\rangle + i|-\alpha\rangle)/N_{\pi/2}$ . The average photon number of  $|\alpha\rangle_{\text{YS}}$  is  $|\alpha|^2$ . Thus, the LZ probability for the YS state becomes

$$P_{\text{LZ}}(\infty) = 1 - P_{\uparrow,0} \exp\left[-|\alpha|^2(1 - P_{\uparrow,0})\right], \quad (11)$$

which reveals the dependence of  $P_{\text{LZ}}(\infty)$  on the ratio  $\Delta^2/v$  and the average photon number  $|\alpha|^2$ . Obviously, enhancing  $|\alpha|^2$  and the ratio  $\Delta^2/v$  will increase the final LZ probability  $P_{\text{LZ}}(\infty)$ .

#### 2. Even coherent state

When  $\theta = 0$ , the photon state is the so-called ‘‘even coherent state’’:  $|\alpha\rangle_+ = (|\alpha\rangle + |-\alpha\rangle)/N_0$ , with  $N_0^2 = 2(1 + e^{-2|\alpha|^2})$ . This state refers to the fact that the photon number distribution is nonzero only for even photon numbers with the average photon number  $\bar{n} = 2|\alpha|^2(1 - e^{-2|\alpha|^2})/N_0^2$ . Then the final probability

$$P_{\text{LZ},+}(\infty) = 1 - P_{\uparrow,0} \frac{\cosh(|\alpha|^2 P_{\uparrow,0})}{\cosh|\alpha|^2}. \quad (12)$$

#### 3. Odd coherent state

When  $\theta = \pi$ , the photon state is an ‘‘odd coherent state’’:  $|\alpha\rangle_- = \frac{1}{N_{\pi}} (|\alpha\rangle - |-\alpha\rangle)$ , with  $N_{\pi}^2 = 2(1 - e^{-2|\alpha|^2})$ , for which only an odd number of photons have

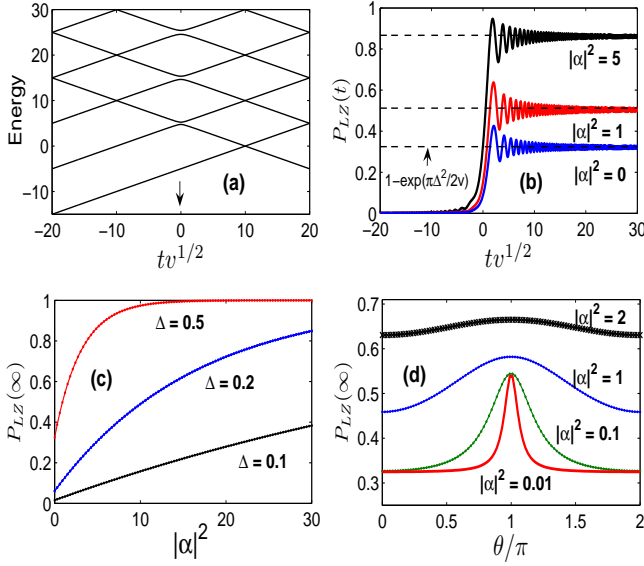


Figure 1: (Color online) (a) Adiabatic energy levels of the quantized LZ Hamiltonian (3) within the RWA. The coupling  $\Delta = 0.5$  and frequency  $\omega = 10$  are both in units of  $\sqrt{v}$ , also  $\hbar = 1$ . The arrow marks the point where the avoided crossings are located. (b) LZ probability  $P_{LZ}(t)$  as a function of time, in units of  $1/\sqrt{v}$ , for the coupling  $\Delta = 0.5$ , and for various values of the average photon number  $|\alpha|^2$ . The horizontal black dashed lines show the analytical results in Eq. (11). (c) Final LZ transition probability  $P_{LZ}(\infty)$  versus average photon number  $|\alpha|^2$  for various couplings  $\Delta = 0.1, 0.2$ , and  $0.5$ . (d) Final LZ probability  $P_{LZ}(\infty)$  as a function of the superposition parameter  $\theta$ , for the coupling  $\Delta = 0.5$  and various values of  $|\alpha|^2$ .

a nonzero probability and the average photon number  $\bar{n} = 2|\alpha|^2(1 + e^{-2|\alpha|^2})/N_\pi^2$ . Then the LZ probability becomes

$$P_{LZ,-}(\infty) = 1 - P_{\uparrow,0} \frac{\sinh(|\alpha|^2 P_{\uparrow,0})}{\sinh |\alpha|^2}. \quad (13)$$

When  $|\alpha|^2$  approaches zero, we have  $P_{LZ,-}(\infty) \rightarrow 1 - P_{\uparrow,0}^2$ , because the odd coherent state  $|\alpha\rangle_-$  tends to the Fock state  $|1\rangle$ .

#### 4. Numerical results of LZ processes for various types of coherent superposition states

Let us first focus on the YS coherent state and numerically study the LZ processes. In Fig. 1 (b), we show that for a weak coupling  $\Delta = 0.5$  (in units of  $\sqrt{v}$ ), the LZ transition occurs near the point  $t = 0$ , at the avoided crossings. The coherent oscillation of  $P_{LZ}(t)$  is enhanced by increasing the average photon number  $|\alpha|^2$ . Figure 1 (c) shows the final probability  $P_{LZ}(\infty)$  as a function of  $|\alpha|^2$  for different couplings  $\Delta$ . As expected in the analytical results, for increasing  $|\alpha|^2$  we find that  $P_{LZ}(\infty)$  tends to

1 monotonically, and larger couplings  $\Delta$  accelerate this increase. The superposition parameter  $\theta$  gives a periodic contribution to  $P_{LZ}(\infty)$ , as shown in Fig. 1 (d). For small average photon numbers  $|\alpha|^2 < 2$ , there is a clear maximum of  $P_{LZ}(\infty)$  at  $\theta = \pi$  (odd coherent state), which implies that not only the average photon number but also the proper superpositions of coherent states can enhance the LZ probabilities. When  $|\alpha|^2$  is larger, however, there is hardly any effect of the superposition parameter  $\theta$ . Then all the superpositions of coherent states provide the same asymptotic value of  $P_{LZ}(\infty)$ , as shown in Fig. 1 (d).

### B. Entanglement between the quantum TLS and the photon field

Due to the coupling terms in the LZ-JC Hamiltonian, the dynamics will produce entanglement between the quantum TLS and the photon field. The aim of this section is to reveal the connection between the LZ transition and the entanglement creation. The concept of purity can be employed to characterize entanglement. Based on the reduced density of TLSs, purity is determined by the linear entropy, defined by  $E_l(t) = 1 - \text{Tr} \rho_{\text{TLS}}^2(t)$ . In terms of the elements of the density matrix, we have  $E_l(t) = 1 - \sum_{i,j=\uparrow,\downarrow} |\langle i | \rho_{\text{TLS}} | j \rangle|^2$ . In the LZ process we find the matrix elements of the density matrix as a function of time

$$\begin{aligned} |\langle \uparrow | \rho_{\text{TLS}} | \downarrow \rangle|^2 &= \frac{-\sin^2 \theta}{N_\theta^2 e^{2|\alpha|^2}} \left| \sum_{n=0}^{\infty} \frac{(-1)^n |\alpha|^{2n+1} A_{n+1} B_n^*}{\sqrt{(n+1)n!}} \right|^2, \\ |\langle \uparrow | \rho_{\text{TLS}} | \uparrow \rangle|^2 &= [1 - P_{LZ}(t)]^2, \\ |\langle \downarrow | \rho_{\text{TLS}} | \downarrow \rangle|^2 &= P_{LZ}^2(t). \end{aligned} \quad (14)$$

Due to the exact solutions of  $A_n(t)$  and  $B_n(t)$ , the linear entropy can be analytically obtained. If we choose even (or odd) coherent states in Eq. (8) for  $\theta = 0$  (or  $\pi$ ), there will be a simple form of the linear entropy

$$E_l(t) = 2P_{LZ}(t)[1 - P_{LZ}(t)], \quad (15)$$

which implies that the TLS and the photon field can achieve full entanglement, in the sense that, after tracing out the photon states, no coherence between  $|\uparrow\rangle$  and  $|\downarrow\rangle$  is left; i.e., the antidiagonal elements in the reduced density matrix of Eq. (14) vanish. In this case, the entanglement is absolutely determined by  $P_{LZ}(t)$ . At finite times, when  $P_{LZ}(t)$  suddenly jumps to a nonzero value but is less than  $1/2$ ,  $E_l(t)$  increases fast to a steady value. However, if  $P_{LZ}(t)$  is larger than  $1/2$ ,  $E_l(t)$  decreases. The entanglement will be less perfect if other initial superposition parameters ( $\theta \neq 0, \pi$ ) are chosen, because there will be nonzero off-diagonal elements in the reduced density matrix. The entanglement dynamics strongly depends on the LZ transition probability, and this is confirmed by the numerical results shown in Fig. 2.

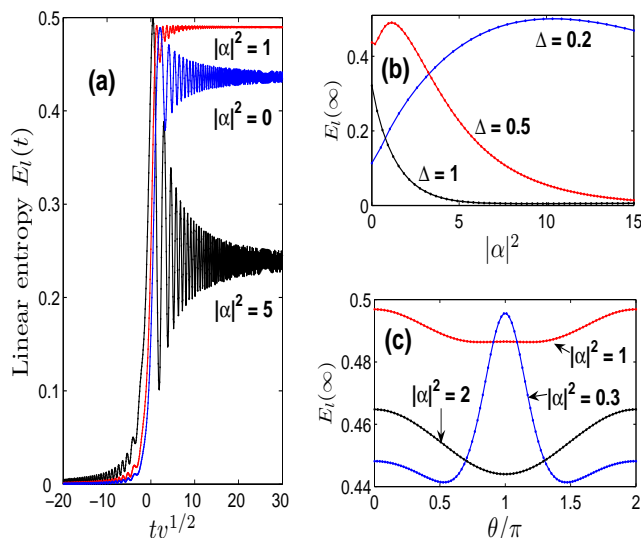


Figure 2: (Color online) (a) Linear entropy  $E_l(t)$  as a function of time (in units of  $1/\sqrt{v}$ ) for the coupling  $\Delta = 0.5$  (in units of  $\sqrt{v}$ ) and for various values of the average photon number  $|\alpha|^2$ . (b) Final or long-time linear entropy  $E_l(\infty)$  as a function of  $|\alpha|^2$ , for various couplings  $\Delta = 0.2, 0.5$ , and  $1$ . (c) Final linear entropy  $E_l(\infty)$  versus the superposition parameter  $\theta$ , for the coupling  $\Delta = 0.5$  and various  $|\alpha|^2$ .

For an initial YS coherent state, the dynamics of the linear entropy  $E_l(t)$  for finite times is shown in Fig. 2 (a). The entanglement between the TLS and the photon field is created when the LZ transition occurs. Analogous to the LZ probability,  $E_l(t)$  oscillates with time and tends to a steady value. However, it is not always the case that the larger  $|\alpha|^2$  is, the stronger the entanglement will be. In Fig. 2 (b), we plot the final linear entropy  $E_l(t = \infty)$  versus  $|\alpha|^2$ . Clearly, for small values of the coupling  $\Delta$ , the linear entropy  $E_l(\infty)$  has a maximum. However, for larger couplings, like  $\Delta = 1$ , increasing  $|\alpha|^2$  only suppresses  $E_l(\infty)$  rapidly. Note that in the large-coupling  $\Delta$  limit,  $P_{LZ}(\infty)$  achieves unity adiabatically, which implies that the final state is separable. In Fig. 2 (c), the linear entropy  $E_l(\infty)$  versus the initial superposition parameter  $\theta$  for a small coupling  $\Delta = 0.5$  is considered. The odd coherent state at  $\theta = \pi$  has a maximal entanglement for a small photon number  $|\alpha|^2 = 0.3$ , whereas it has a minimal entanglement for a larger photon number  $|\alpha|^2 = 2$ .

### C. Photon distribution of the field

One of the best-known nonclassical effects is the generation of sub-Poissonian (or super-Poissonian) photon statistics of the light field [45, 46]. A coherent state  $|\alpha\rangle$ , which can be regarded as a state with the “most” classical behavior, yields a Poissonian distribution, i.e., the variance of the number operator  $\hat{n} = a^\dagger a$  is equal to the mean

photon number:  $(\Delta\hat{n})^2 = \bar{n} = |\alpha|^2$ . Mandel introduced the  $Q$  parameter [45],

$$Q = \frac{(\Delta n)^2}{\bar{n}} - 1, \quad (16)$$

which characterizes the departure from the Poissonian distribution, i.e., the nonclassical property. When  $Q = 0$ , the state is called Poissonian, while, for  $Q > 0$  the state is super-Poissonian. If  $-1 \leq Q < 0$ , the statistics is sub-Poissonian. It is known that the Yurke-Stoler coherent state is Poissonian. However, under time evolution, the parameter  $Q$  changes with time as  $Q(t) = (\Delta\hat{n})^2_t / \bar{n}_t - 1$ . Thus the initial Poissonian may turn into sub-Poissonian or super-Poissonian. It is interesting to consider how the photon distribution changes during the LZ process.

For the superposition of coherent states in Eq. (8), at finite times, we obtain the average photon number

$$\bar{n}_t = \bar{n}_0 + P_{LZ}(t), \quad (17)$$

where  $\bar{n}_0 = 2|\alpha|^2(1 - e^{-2|\alpha|^2} \cos\theta) / N_\theta^2$  indicates the initial average photon number. The expression given above reflects that the dynamics of  $\bar{n}_t$  is dominated by the LZ transition probability  $P_{LZ}(t)$ . The asymptotic behavior at infinite time will be  $\bar{n}_\infty = \bar{n}_0 + P_{LZ}(\infty)$ . We also obtain the average value of  $\hat{n}^2$  at  $t = \infty$ ,

$$\langle \hat{n}^2 \rangle_\infty = \frac{-4|\alpha|^2 P_{\uparrow,0}^2}{N_\theta^2 e^{|\alpha|^2}} \left( e^{|\alpha|^2 P_{\uparrow,0}} - e^{-|\alpha|^2 P_{\uparrow,0} \cos\theta} \right) + |\alpha|^4 + 3\bar{n}_0 + P_{LZ}(\infty), \quad (18)$$

where  $P_{LZ}(\infty)$  is shown in Eq. (10). By the definition in Eq. (16), the asymptotic value of  $Q(t)$  becomes  $Q(\infty) = (\Delta\hat{n})^2_\infty / \bar{n}_\infty - 1$ , where the variance  $(\Delta\hat{n})^2_\infty = \langle \hat{n}^2 \rangle_\infty - \bar{n}_\infty^2$ . We shall now concentrate on some limiting cases: (i) when  $|\alpha|^2 = 0$ , for finite LZ rate  $\Delta^2/v \neq 0$ , we have  $Q(\infty) < 0$ , i.e., the LZ transition induces sub-Poissonian statistics in the photon field; and (ii) when  $|\alpha|^2$  is very large, we have  $Q(\infty) \rightarrow 0$ , in which case the LZ transition has no effect on the photon distribution.

In Fig. 3 (a), we numerically plot the Mandel parameter  $Q(t)$  versus time  $t$ . Obviously, the photon statistics of the field changes suddenly when the LZ transition occurs. Near the avoided-level-crossing point, for  $|\alpha|^2 > 0$ , super-Poissonian and sub-Poissonian statistics appear alternately. The final Mandel parameter  $Q(\infty)$  versus  $|\alpha|^2$  is shown in Fig. 3 (b), for weak couplings  $\Delta$ , both sub-Poissonian and super-Poissonian statistics can appear with increasing  $|\alpha|^2$ . For the large  $|\alpha|^2$  limit, the photon distribution finally tends to Poissonian, which is not shown here. We also show  $Q(\infty)$  versus the LZ parameter  $\Delta/\sqrt{v}$  in Fig. 3 (c). When  $|\alpha|^2 = 0$ ,  $Q$  monotonically decays with  $\Delta/\sqrt{v}$  from 0 to  $-1$ , whereas, for a finite average photon number such as  $|\alpha|^2 = 1$ , super-Poissonian statistics also appears. However, a large  $|\alpha|^2$  will erase the nonclassical effects revealed by the sub-Poissonian (or super-Poissonian).

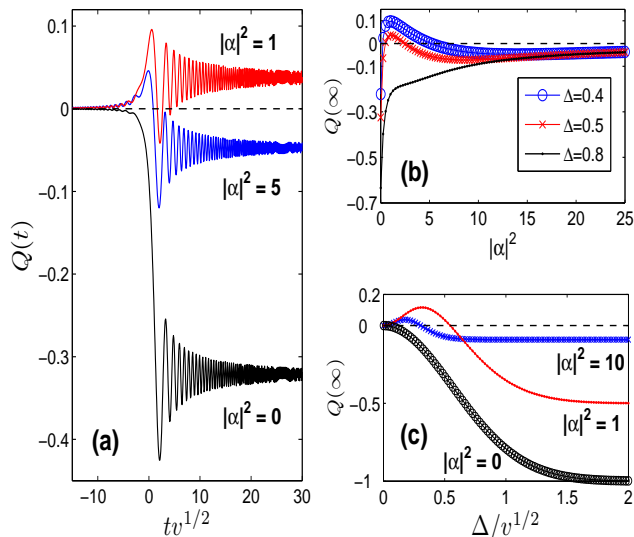


Figure 3: (Color online) (a) Mandel parameter  $Q(t)$  as a function of time in units of  $1/\sqrt{v}$  for various values of the average photon number  $|\alpha|^2$  and the coupling  $\Delta = 0.5$  in units of  $\sqrt{v}$ . (b) Final Mandel parameter  $Q(\infty)$  as a function of  $|\alpha|^2$  for various couplings  $\Delta = 0.2, 0.5$ , and  $1$ . (c) Final  $Q(\infty)$  versus coupling  $\Delta$  for various  $|\alpha|^2$ . The horizontal black dashed lines mark  $Q = 0$  and correspond to a Poissonian distribution.

#### IV. LANDAU-ZENER TRANSITION WITHOUT THE RWA

In this section, we consider the LZ transition *without* the RWA. A reasonable comparison between the solutions with and without the RWA will enable us to understand the contribution from the counter-rotating terms.

##### A. YS coherent state case

Without the RWA, due to the counter-rotating terms  $\sigma_+ a^\dagger$  and  $\sigma_- a$ , the total number operator  $\hat{N} = a^\dagger a + \sigma_z/2$  is not conserved by the Hamiltonian in Eq. (2), i.e.,  $[\hat{N}, H] \neq 0$ . Then the Hamiltonian (2) cannot be exactly diagonalized and has a fundamentally different energy structure from the Hamiltonian (3) within the RWA, no matter how small the coupling  $\Delta$  is. From the adiabatic energy spectrum in Fig. 4 (a), clearly, one can find two groups of avoided-level crossings, which are significantly different from the RWA case in Fig. 1 (a). The groups of avoided-level crossing are formed not only between the states  $|\uparrow n\rangle$  and  $|\downarrow n+1\rangle$  but also between  $|\uparrow n\rangle$  and  $|\downarrow n-1\rangle$  (when  $n \geq 2$ ), with level splittings  $\Delta\sqrt{n+1}$  and  $\Delta\sqrt{n}$ , respectively. Note that the two groups of avoided crossings are approximately independent whenever the time between the successive avoided level crossings,  $t_{\text{cross}} = 2\omega/v$ , exceeds the duration of an individual LZ transition,  $\tau_{\text{LZ}} \sim \max\{1/\sqrt{v}, \Delta/v\}$  [47, 48]. For our multilevel LZ problem, the couplings

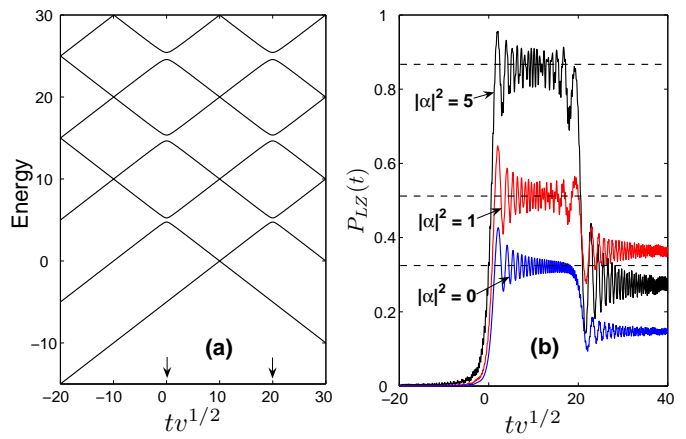


Figure 4: (Color online) (a) Adiabatic energy levels of the quantized LZ Hamiltonian (2) without RWA. The coupling  $\Delta = 0.5$ , frequency  $\omega = 10$ , and the parameters are in units of  $\sqrt{v}$ . The vertical arrows show the points where the avoided crossings are located. (b) LZ probability  $P_{\text{LZ}}(t)$  as a function of time (in units of  $1/\sqrt{v}$ ) for various values of the average photon number  $|\alpha|^2$ , and for the coupling  $\Delta = 0.5$  and frequency  $\omega = 10$ . The horizontal black dashed lines show the analytical results of Eq. (11) with the RWA which, in the middle, approximately agree with the first-stage LZ transitions.

become  $\Delta_n = \Delta\sqrt{n+1}$  (or  $\Delta\sqrt{n}$ ). Thus the “independent LZ transition approximation” holds as long as the Fock states  $|n\rangle$ , with  $n > 4\omega^2/\Delta^2$ , are not occupied, i.e., when  $\omega > \max\{\sqrt{v}/4, |\alpha|\Delta\}$ .

The appearance of the second set of avoided-level crossings then allows the occurrence of the second transition. Therefore, two stages of the LZ transition are predictable and numerically shown in Fig. 4 (b). We choose  $\omega = 10$  and  $\Delta = 0.5$  (in units of  $\sqrt{v}$ ), and then there exist two (almost) independent LZ transitions. The second transitions just occur in the vicinity of the second set of avoided crossings at  $t = 2\omega/v$ . The analytical results for  $P_{\text{LZ}}(\infty)$  [in Eq. (11)] within the RWA are marked by dashed lines. For different  $|\alpha|^2$  cases, the first-stage LZ probabilities nicely agree with the RWA results. However, after the second stage, the final LZ probabilities significantly deviate from the RWA results.

In order to reveal the richness of the dynamics without the RWA, in Fig. 5, we have numerically calculated LZ probabilities for  $|\alpha|^2 = 1$  and various values of the couplings  $\Delta$  and frequencies  $\omega$ . Obviously, once small frequencies such as  $\omega = 1$  are chosen, the time  $t_{\text{cross}} = 2\omega/v$  is of the order  $\tau_{\text{LZ}}$ , where the two LZ transitions start to interfere with each other. By increasing the frequency  $\omega$ , there are two visible stages of the LZ transition. The first-stage LZ probabilities do not depend strongly on the frequency  $\omega$ , as long as  $|\alpha|\Delta \ll \omega$  is satisfied. However, the second-stage LZ probability is influenced strongly by the frequencies  $\omega$ .

If all the avoided crossings are well separated, we can approximately treat the transitions as being independent and compute the transition probabilities as joint proba-

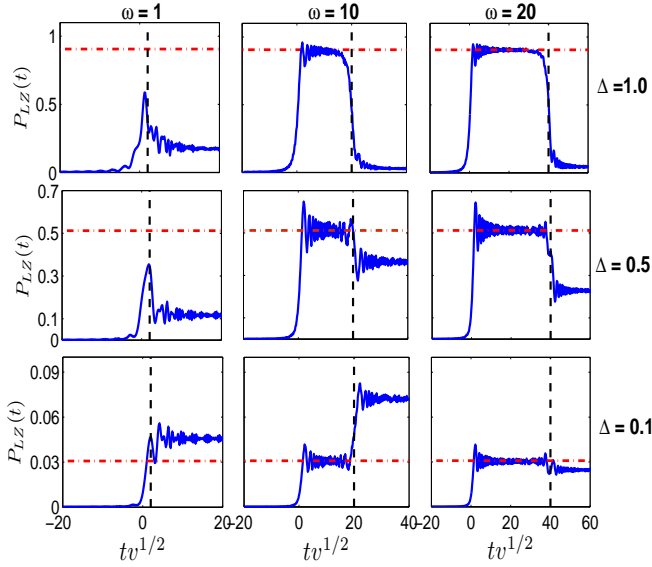


Figure 5: (Color online) LZ transition probability  $P_{LZ}(t)$  as a function of time (in units of  $1/\sqrt{v}$ ) and various values of the coupling  $\Delta$  (in units of  $\sqrt{v}$ ) and frequency  $\omega$  (in units of  $\sqrt{v}$ ). The average photon number  $|\alpha|^2 = 1$ . The horizontal red dash-dot lines show the analytical results of Eq. (11) within the RWA. The vertical black dashed lines indicate the times between the successive avoided-level crossings, i.e., the two stages of the LZ transitions.

bilities [28, 48, 49]. For the Hamiltonian (2) without the RWA, the final probability to find the TLS at  $|\uparrow\rangle$  from the initial state  $|\uparrow n\rangle$  is [49]

$$P_{\uparrow, n \rightarrow \uparrow} = P_{\uparrow, n-1} P_{\uparrow, n} + (1 - P_{\uparrow, n-1})(1 - P_{\uparrow, n-2}), \quad (19)$$

where  $P_{\uparrow, n} = \exp[-\pi\Delta^2(n+1)/2v] = P_{\uparrow, 0}^{n+1}$ , and the expanded form of the equation above still holds for the  $n = 0$  and 1 cases. By substituting  $P_{\uparrow, n \rightarrow \uparrow}$  into  $P_{LZ}(\infty) = 1 - \sum_{n=0}^{\infty} |C_n|^2 P_{\uparrow, n \rightarrow \uparrow}$ , we obtain the LZ probability in the independent-transition approximation and weak couplings:

$$P_{LZ}(\infty) = \frac{K_{\alpha, \theta}}{P_{\uparrow, 0}} [f_{\alpha, \theta}(P_{\uparrow, 0}) - f_{\alpha, \theta}(P_{\uparrow, 0}^2)], \quad (20)$$

where the coefficient  $K_{\alpha, \theta} = e^{-|\alpha|^2}/(1 + \cos\theta e^{-2|\alpha|^2})$  depends on  $|\alpha|^2$  and  $\theta$ . The function  $f_{\alpha, \theta}$  is defined by  $f_{\alpha, \theta}(x) = (1+x) \left( e^{|\alpha|^2 x} + \cos\theta e^{-|\alpha|^2 x} \right)$ . When  $|\alpha|^2 \rightarrow 0$ , for  $\cos\theta \neq -1$ , we find that  $P_{LZ}(\infty)$  tends to the standard LZ probability  $1 - P_{\uparrow, 0}$ , whereas, for  $\cos\theta = -1$ ,  $P_{LZ}(\infty)$  approaches  $1 - P_{\uparrow, 0}^3$ . In the large photon number limit  $|\alpha|^2 \rightarrow \infty$ , Eq. (20) gives  $P_{LZ} \rightarrow 0$ .

By performing a numerical time integration for  $t \in [-50, 50]$ , in units of  $1/\sqrt{v}$ , we calculate the long-time LZ probability as a function of  $|\alpha|^2$  for different values of  $\Delta$ ; these results are shown in Fig. 6 (a). Clearly, the LZ probability possesses a nonmonotonic behavior. When the coupling is sufficiently weak, such as  $\Delta = 0.1$ , the

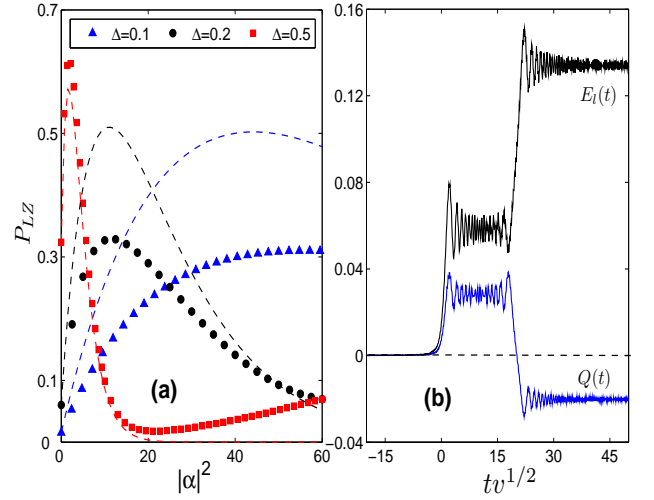


Figure 6: (Color online) (a) Without the RWA, the long-time LZ probability  $P_{LZ}$  as a function of  $|\alpha|^2$  for different couplings  $\Delta$ , in units of  $\sqrt{v}$ . The frequency  $\omega = 10$  (in units of  $\sqrt{v}$ ) and the numerical time integration is performed over  $[-50, 50]$ . The blue solid triangles, black solid circles and red solid squares denote the numerical results for  $\omega = 0.1, 0.2$ , and  $0.5$ , respectively. The dashed lines correspond to the analytical results of Eq. (20), and the blue, black and red lines denote  $\omega = 0.1, 0.2$  and  $0.5$ , respectively. (b) Linear entropy  $E_L(t)$  and Mandel parameter  $Q(t)$  as a function of time (in units of  $1/\sqrt{v}$ ). The average photon number is  $|\alpha|^2 = 1$ , the coupling  $\Delta = 0.1$ , and the frequency  $\omega = 10$ , in units of  $\sqrt{v}$ .

LZ probability increases with  $|\alpha|^2$  monotonically in quite a long region of  $|\alpha|^2$ . However, a stronger coupling like  $\Delta = 0.5$  makes the LZ probability achieve a maximum value quickly. Unfortunately, the approximate result in Eq. (20) is not in good agreement with the numerical results, which is unlike the thermal state case [49]. This is because the initial photon state is of Poissonian (sub- or super-) statistics, and the independent-transition condition  $\omega > \max\{\sqrt{v}/4, |\alpha|\Delta\}$ , will be destroyed by increasing  $|\alpha|$ . Moreover, the LZ process strongly depends on the frequencies  $\omega$  even in the weak-coupling region (see Fig. 5). Nevertheless, the approximation result of Eq. (20) still indicates a significant fact that the long-time LZ probability no longer increases monotonously with the photon number  $|\alpha|^2$ .

In Fig. 6 (b), the dynamics of entanglement and Mandel parameter  $Q$  can also present two transitions. From all the numerical results shown in Figs. 4–6, we find that there are some qualitative differences between the results within and without the RWA. Nevertheless, under certain conditions, the RWA results are in good agreement with the first-stage LZ transition. Thus one can choose properly weak couplings  $\Delta$  and large frequencies  $\omega$  to extend the time interval between the two LZ transitions, when the RWA is valid.

For comparison, we also consider the thermal state case, and below we calculate the LZ probability with the

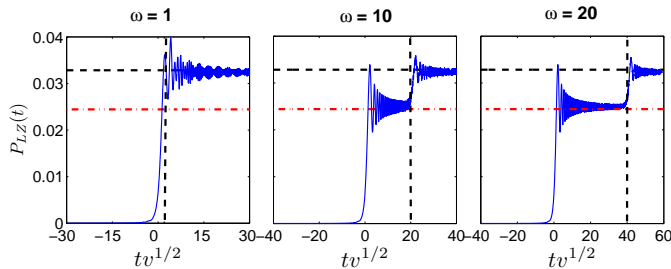


Figure 7: (Color online) The initial state of the photon field is now a thermal state. Without the RWA, we plot the LZ probability  $P_{LZ}(t)$  as a function of time in units of  $1/\sqrt{v}$  for various frequencies  $\omega = 1, 10,$  and  $20$ , in units of  $\sqrt{v}$ . The coupling  $\Delta = 0.1$  in units of  $\sqrt{v}$ , and the scaled temperature  $T/\omega = 1$ . The horizontal red dash-dot lines mark the analytical results in Eq. (22) with the RWA, and the horizontal black dashed line corresponds to the analytical results in Eq. (23) without the RWA. The vertical dashed lines indicate the time between the successive two stages of the LZ transitions.

RWA and without the RWA.

### B. Thermal state case

When the photon field initially starts from a thermal state, the density matrix of the total system is

$$\rho_{\text{tot}}(0) = |\uparrow\rangle\langle\uparrow| \otimes \frac{1}{Z} \exp(-\omega a^\dagger a/T), \quad (21)$$

where the partition function  $Z = (1 - e^{-\omega/T})^{-1}$  (setting  $\hbar, k_B = 1$ ). Within the RWA, the final LZ transition probability becomes

$$P_{LZ}(\infty) = \frac{1 - P_{0,LZ}}{1 + \bar{n}P_{0,LZ}}, \quad (22)$$

where the average photon number  $\bar{n} = [\exp(\omega\beta) - 1]^{-1}$ , and  $P_{0,LZ}$  denotes the standard LZ probability:  $P_{0,LZ} = 1 - \exp(-\pi\Delta^2/2v)$ . When the scaled temperature  $T/\omega \rightarrow 0$ , we find that  $P_{LZ}(\infty)$  tends to the standard LZ probability.

Without the RWA, the approximate final LZ transition probability for finite temperature and weak coupling becomes [49]

$$P_{LZ}(\infty) = \frac{G_T}{P_{\uparrow,0}} [f_T(P_{\uparrow,0}) - f_T(P_{\uparrow,0}^2)], \quad (23)$$

where  $G_T = 1 - \exp(-\omega/T)$ , and the function  $f_T(x) = [1 - x \exp(-\omega/T)]^{-1}$ . For the initial thermal state, the probability  $p(n)$  of finding  $n$  photons is exponentially dependent on  $\omega$ , which is quite different from the case of the YS coherent state, where the photon distribution is Poissonian and independent of  $\omega$ . Consequently, in Fig. 7, for an initial thermal state, we plot the LZ probability versus time for weak coupling  $\Delta$ . The first-stage LZ probability

is consistent with the RWA results, and the second-stage LZ transitions also confirm the approximate results of Eq. (23). Moreover, for different frequencies  $\omega$ , although the curves differ strongly around  $t = 0$ , the LZ probabilities converge toward the same value, which is significantly different from the case of the YS coherent state, where the LZ probabilities strongly depend on  $\omega$  and do not converge to a single value (see Fig. 5).

## V. CONCLUSIONS

We have investigated the LZ transition in a composite system of a TLS coupled to a single-mode photon field. The initial state of the field was chosen as a superposition of coherent states. Within the RWA, we analytically obtained the LZ probability as a function of the average photon number and the superposition parameter. By increasing the average photon number and choosing proper superposition parameters, one can enhance the LZ probability. We also found that both the creation entanglement (between the TLS and field) and the photon distribution change drastically when the LZ transitions occur, which is helpful for revealing the effects of the LZ transition on the whole quantum system.

Beyond the RWA, we found some qualitative differences from the RWA results. The final LZ probability no longer monotonically depends on the average photon number. In addition, two obvious stages of the LZ transition appear in the vicinity of the successive avoided crossings, and the RWA results can only indicate the first-stage LZ probability. The final LZ probability, after the second stage, significantly deviates from the RWA results and strongly depends on the frequencies  $\omega$ , even for weak couplings  $\Delta$ .

We found that the LZ dynamics is quite different from the thermal state case, which is due to the Poissonian distribution in the superposition of coherent states. Although the RWA fails in estimating the final LZ probability, it plays an important role in characterizing the finite-time coherent oscillations generated by the LZ transitions. With sufficiently weak coupling  $\Delta$  and large frequency  $\omega$ , one can extend the time interval between the two LZ transitions when the RWA is accurate enough. Very recently, the authors of Ref. [50] found the absence of vacuum-induced Berry phases without the RWA. Our results also provide examples indicating that the RWA leads to faulty results.

### Acknowledgments

We would like to thank S. N. Shevchenko for useful discussions. X.G.W. acknowledges support from the NFRPC under Grant No. 2012CB921602 and from the NSFC under Grant No. 11025527 and No. 10935010. F.N. is partially supported by the ARO, NSF Grant No. 0726909, JSPS-RFBR Contract No. 12-02-92100, Grant-



in-Aid for Scientific Research (S), MEXT Kakenhi on Quantum Cybernetics, and the JSPS via its FIRST program. Z.S. acknowledges support from the NSFC under Grant No. 11005027, the Natural Science Foundation of Zhejiang Province with Grant No. Y6090058, and Pro-

gram for HNUEYT under Grant No. HNUEYT 2011-01-011. J.M. acknowledges support from the Scholarship Award for Excellent Doctoral Student granted by the Ministry of Education.

- 
- [1] S. Shevchenko, S. Ashhab, and F. Nori, *Phys. Rep.* **492**, 1 (2010).
- [2] S. Gasparinetti, P. Solinas, and J. P. Pekola, *Phys. Rev. Lett.* **107**, 207002 (2011).
- [3] C. Kasztelan *et al.*, *Phys. Rev. Lett.* **106**, 155302 (2011).
- [4] J.-N. Zhang, C. P. Sun, S. Yi, and F. Nori, *Phys. Rev. A* **83**, 033614 (2011).
- [5] S. Ashhab, J. R. Johansson, and F. Nori, *Phys. Rev. A* **74**, 052330 (2006).
- [6] L. Tian, S. Lloyd, and T. P. Orlando, *Phys. Rev. B* **65**, 144516 (2002).
- [7] J. M. Martinis, *et al.*, *Phys. Rev. Lett.* **95**, 210503 (2005).
- [8] Y.-A. Chen, S. D. Huber, S. Trotzky, I. Bloch, and E. Altman, *Nat. Phys.* **7**, 61 (2011).
- [9] M. G. Bason *et al.*, *Nat. Phys.* **8**, 147 (2012).
- [10] D. M. Berns *et al.*, *Nature (London)* **455**, 51 (2008).
- [11] A. Zenesini *et al.*, *Phys. Rev. Lett.* **103**, 090403 (2009).
- [12] J.Q. You and F. Nori, *Physics Today* **58** (11), 42 (2005).
- [13] J.Q. You and F. Nori, *Nature (London)* **474**, 589 (2011).
- [14] I. Buluta, S. Ashhab, and F. Nori, *Reports on Progress in Physics* **74**, 104401 (2011).
- [15] P.D. Nation, J.R. Johansson, M.P. Blencowe, and F. Nori, *Rev. Mod. Phys.* **84**, 1-24 (2012).
- [16] A. Izmailkov *et al.*, *Europhys. Lett.* **65**, 844 (2004).
- [17] W. D. Oliver *et al.*, *Science* **310**, 1653 (2005).
- [18] M. Sillanpää *et al.*, *Phys. Rev. Lett.* **96**, 187002 (2006).
- [19] C. M. Wilson *et al.*, *Phys. Rev. Lett.* **98**, 257003 (2007).
- [20] A. Izmailkov *et al.*, *Phys. Rev. Lett.* **101**, 017003 (2008).
- [21] G. Z. Sun *et al.*, *Nat. Commun.* **1**, 51 (2010).
- [22] A.V. Shytov, *Phys. Rev. A* **70**, 052708 (2004).
- [23] K. Saito, M. Wubs, S. Kohler, P. Hänggi, and Y. Kayanuma, *Europhys. Lett.* **76**, 22 (2006).
- [24] A. Altland and V. Gurarie, *Phys. Rev. Lett.* **100**, 063602 (2008).
- [25] M. Wubs *et al.*, *New J. Phys.* **7**, 218 (2005).
- [26] J. Keeling and V. Gurarie, *Phys. Rev. Lett.* **101**, 033001 (2008).
- [27] M. Wubs, K. Saito, S. Kohler, P. Hänggi, and Y. Kayanuma, *Phys. Rev. Lett.* **97**, 200404 (2006).
- [28] K. Saito, M. Wubs, S. Kohler, Y. Kayanuma, and P. Hänggi, *Phys. Rev. B* **75**, 214308 (2007).
- [29] P. Nalbach and M. Thorwart, *Phys. Rev. Lett.* **103**, 220401 (2009).
- [30] P. P. Orth, A. Imambekov, and K. Le Hur, *Phys. Rev. A* **82**, 032118 (2010).
- [31] R. S. Whitney, M. Clusel, and T. Ziman, *Phys. Rev. Lett.* **107**, 210402 (2011).
- [32] W. H. Zurek, *Rev. Mod. Phys.* **75**, 715 (2003).
- [33] A. Ourjoumtsev *et al.*, *Science* **312**, 83 (2006).
- [34] A. Ourjoumtsev *et al.*, *Nature (London)* **448**, 784 (2007).
- [35] A. P. Lund, T. C. Ralph, and H. L. Haselgrove, *Phys. Rev. Lett.* **100**, 030503 (2008).
- [36] S. J. van Enk and O. Hirota, *Phys. Rev. A* **64**, 022313 (2001).
- [37] I. Afek, O. Ambar, Y. Silberberg, *Science* **328**, 879 (2010).
- [38] J. Joo, W. J. Munro, and T. P. Spiller, *Phys. Rev. Lett.* **107**, 083601 (2011).
- [39] J. Larson and S. Stenholm, *J. of Mod. Optics* **50**, 1663 (2003).
- [40] J. Larson, *Physica Scripta* **76**, 146 (2007).
- [41] J. Majer *et al.*, *Nature (London)* **449**, 443 (2007).
- [42] T. Niemczyk *et al.*, *Nat. Phys.* **6**, 772 (2010).
- [43] B. Yurke and D. Stoler, *Phys. Rev. Lett.* **57**, 13 (1986).
- [44] A. Sarlette *et al.*, *Phys. Rev. Lett.* **107**, 010402 (2011).
- [45] L. Mandel, *Opt. Lett.* **4**, 205 (1979).
- [46] W. Choi *et al.*, *Phys. Rev. Lett.* **96**, 093603 (2006).
- [47] K. Mullen, E. Ben-Jacob, Y. Gefen, and Z. Schuss, *Phys. Rev. Lett.* **62**, 2543 (1989).
- [48] A. T. S. Wan *et al.*, *Int. J. Quantum Inf.* **7**, 725 (2009).
- [49] D. Zueco, P. Hänggi, and S. Kohler, *New J. Phys.* **10**, 115012 (2008).
- [50] J. Larson, *Phys. Rev. Lett.* **108**, 033601 (2012).